Plankton Benthos Res 19(4): 191–202, 2024

Plankton & Benthos Research

Effects of temperature and light intensity on growth in *Prorocentrum* cf. *balticum* (Dinophyceae) isolated from the Oyashio-Kuroshio Mixed Water region, North Pacific

Chiho Funaki[1], Koyo Kuwata[2], Wai Mun Lum[2,†], Kazuya Takahashi[2,‡],
Takako Masuda[3], Mutsuo Ichinomiya[4], Tomoyo Katayama[1], Taketoshi Kodama[1],
Mitsunori Iwataki[2] & Kazutaka Takahashi[1,*]

[1] *Department of Aquatic Bioscience, Graduate School of Agricultural and Life Sciences, The University of Tokyo, 1–1–1 Yayoi, Bunkyo, Tokyo 113–8657, Japan*
[2] *Asian Research Center for Bioresource and Environmental Sciences, Graduate School of Agricultural and Life Sciences, The University of Tokyo, 1–1–1 Yayoi, Bunkyo, Tokyo 113–8657, Japan*
[3] *Japan Fisheries Research and Education Agency, 3–27–5 Shinhama-cho, Shiogama, Miyagi 985–0001, Japan*
[4] *Faculty of Environmental and Symbiotic Sciences, Prefectural University of Kumamoto, 3–1–100 Tsukide, Kumamoto 862–8502, Japan*
† *Present address: Department of Marine Resources, Graduate School and Faculty of Bioresources, Mie University, 1577 Kurimamachiya, Tsu, Mie 514-8507, Japan*
‡ *Present address: Institute of Parasitology, Biology Centre, Czech Academy of Sciences, 370 05 České Budějovice, Czech Republic*

Received 12 February 2024; Accepted 29 August 2024 Responsible Editor: Toshiya Katano

doi: 10.3800/pbr.19.191

Abstract: Owing to its particular mixotrophic nutrition, *Prorocentrum* cf. *balticum* has recently been suggested to contribute significantly to the biological pump in the world's oceans. However, the physiological attributes that facilitate its distribution have not yet been investigated. We clarified the effects of temperature and light intensity on the growth of a strain of *P.* cf. *balticum* isolated from the Oyashio-Kuroshio Mixed Water region and then estimated its potential habitat in the western North Pacific in the context of global warming. In batch cultures maintained at 5°C–30°C, the highest growth was observed at 25°C, while the viable temperature range was estimated to be 6.03°C–29.4°C. At the six different light conditions tested (20–500 μmol m^{-2} s^{-1}), growth rates were positively correlated with light intensity, except at 500 μmol m^{-2} s^{-1} where photoinhibition was observed. At 20°C, the maximum specific growth rate was calculated to be 0.661 day^{-1} and the compensation light intensity and the saturation light intensity were 1.15 and 283 μmol m^{-2} s^{-1}, respectively. These findings suggested that compared to other *Prorocentrum* species, *P.* cf. *balticum* is generally well suited to subtropical environments characterized by high light intensities. However, the potential to survive in mid-latitude environments that experience low temperatures during winter suggests a high probability of year-round occurrence at higher latitudes, including the Oyashio region, in the future.

Key words: *Prorocentrum balticum*, specific growth rate, temperature, light intensity, potential habitat, global warming

---

1. Introduction

Dinoflagellates belonging to the genus *Prorocentrum* Ehrenberg comprise a diverse group of predominantly marine species that inhabit both benthic and planktonic environments in the world's oceans (Glibert et al. 2012). The ecology and physiology of this group have been particularly well studied in coastal waters because the genus contains species that form intensive blooms (Heil et al. 2005, Lu et al. 2022, Tenorio et al. 2022) and are capable of producing toxins that are responsible for shellfish poi-

---

[*] Corresponding author: Kazutaka Takahashi; E-mail, kazutakahashi@g.ecc.u-tokyo.ac.jp
Supplementary materials may be found in the online version of this article.

soning (Glibert et al. 2012, Lee et al. 2016). On the other hand, from a food web perspective, *Prorocentrum* species are preyed upon by zooplankton such as ciliates and copepods (Ianora et al. 2003, Sakka et al. 2000, Uye 1996). In addition, some *Prorocentrum* species are constitutive mixotrophs (Mitra et al. 2023), that possess the innate ability to photosynthesize as well as synergistically combine both phototrophic and phagotrophic feeding strategies in order to utilize other protists and bacteria (Stoecker et al. 1997, Wikfors & Fernandez 2013). Several studies have emphasized the important role that mixotrophy plays in maintaining the robustness and productivity of the food web, especially in oligotrophic ocean areas (Hartmann et al. 2012, Ward & Follows 2016).

Prorocentrum balticum (Lohmann) Loeblich III, originally described as *Exuviaella baltica* Lohmann from Kiel, Germany (Lohmann 1908), has been widely reported to be a bloom-forming species in coastal regions of the world (Vrquez & Hargraves 1995, O'Boyle et al. 2001, Alonso-Rodriguez & Ochoa 2004, Widdicombe et al. 2010, Telesh et al. 2016, Salon-Barros et al. 2016). It has been distinguished from the other common species *Prorocentrum cordatum* (Ostenfeld) Dodge (=*Prorocentrum minimum* (Pavillard) Schiller) based mainly on the cell shape and size, i.e., *P. balticum* is rather roundish compared to the heart-shaped *P. cordatum* (e.g., Faust et al. 1999, Tillmann et al. 2023a, 2023c). However, recent molecular phylogeny showed further discernible clades in the monophyletic spiny-surfaced *Prorocentrum*, and some were described as new species, such as *Prorocentrum pervagatum* Tillmann, Hoppenrath & Gottschling, *Prorocentrum spinulentum* Tillmann, Gottschling & Hoppenrath, and *Prorocentrum thermophilum* F.Gómez, Tangcheng Li, Hu. Zhang & Senjie Lin, with detailed comparisons of thecal morphology (Gómez et al. 2022, 2023, Tillmann et al. 2023a, 2023c), while other clades remain undescribed such as *Prorocentrum* cf. *balticum* (Larsson et al. 2022).

Recently, Larsson et al. (2022) reported that a strain of *P.* cf. *balticum* isolated from southeastern Australia employs a remarkable feeding strategy that involves crafting globular mucus traps (mucosphere) to capture and immobilize potential prey. The authors proposed that the strain may play an important ecological role in the biological pump since the mucosphere, which is created around the cell using fixed carbon derived from photosynthesis, is subsequently abandoned with surplus prey cells and sinks to depth (Larsson et al. 2022). Their findings highlight the importance of obtaining ecological and physiological information on the strain of *P.* cf. *balticum* in order to understand both ocean carbon cycling as well as the marine food web in subtropical waters, which is expanding poleward as global warming progresses (Polovina et al. 2011, Yang et al. 2020).

In this study, we attempted to clarify the effects of temperature and light intensity on the growth and photosynthesis of *P.* cf. *balticum* and examine how these factors affect its distribution. *Prorocentrum* cf. *balticum* was isolated from the Oyashio-Kuroshio Mixed Water region in the North Pacific and subsequently confirmed to belong to the same phylogenetic clade as the strain *P.* cf. *balticum* reported by Larsson et al. (2022). Based on the results of laboratory experiments, we inferred the potential habitat requirements of *P.* cf. *balticum* to ascertain the northernmost limit of this species in the study area, and how this distribution may be affected by global warming.

2. Materials and Methods

2.1 Culture establishment and species identification

The dinoflagellate strain used in the current experiments was isolated from a seawater sample collected at a depth of 10 m (temperature: 18.6°C, salinity: 33) off the Pacific coast of northeastern Japan (39°30.040′N, 146°30.010′E) during a cruise aboard the *R/V Wakataka-Maru* in July 2022. A monoclonal culture strain was established by capillary pipetting under an inverted microscope (CKX53, Olympus, Tokyo, Japan). The batch culture was maintained in half-strength IMK medium (Wako, Tokyo, Japan) at 23°C and a salinity of 30 under a photon density of 60–70 μmol m^{-2} s^{-1} with a 12 h : 12 h light : dark cycle.

Morphological characteristics of the established strain KWT167 were observed using a Zeiss Axioskop 2 light microscope (Carl Zeiss, Göttingen, Germany) equipped with a Zeiss Axiocam 305 color digital camera. Production of mucosphere (Larsson et al. 2022) was confirmed by coculturing with *Rhodomonas salina* (Wislouch) D.R.A.Hill & R.Wetherbee which is regularly maintained in our laboratory of the University of Tokyo. For molecular phylogeny, several cultured cells were isolated and placed into distilled water, and PCR was performed using the disrupted cells as a template. The primers used to amplify the LSU rDNA (28S rDNA) sequence, the reaction mix, and settings used for PCR, and the subsequent purification and sequencing processes were in accordance with Kuwata et al. (2023). The determined DNA sequence (accession number LC779631 for KWT167 strain) was aligned with those of *Prorocentrum* species obtained from GenBank, and phylogenetic trees of maximum likelihood (ML) and neighbor-joining (NJ) were constructed in MEGA 11 (Stecher et al. 2020, Tamura et al. 2021). The selected best substitution model for ML was the Tamura-Nei (TN93) model plus gamma distribution (G=0.5312). Bootstrap support (BS) values of ML and NJ analyses were estimated using 500 replicates and are given at nodes (ML/NJ).

2.2 Temperature experiments

To investigate the effect of temperature on the growth of the strain KWT 167, batch culture experiments were performed using five different temperature treatments (10, 15, 20, 25, and 30°C) under a constant light intensity of 200 μmol m^{-2} s^{-1}. Before initiating the experiment, cells were pre-acclimatized to the selected temperatures through stepwise changes in temperature of 2.5°C every two days. After acclimation, cells in the exponential growth phase were inoculated into 50 mL of fresh medium to achieve initial cell densities of approximately 100 cells mL^{-1} in each flask. The experiment was performed in triplicate for each temperature condition until a decline in cell density was observed after reaching the maximum cell density. Furthermore, to assess the growth response at lower temperatures, an additional experiment was carried out at 5°C using the same experimental settings as described previously, except for the light intensity, which was set to 100 $\mu\mathrm{mol\,m^{-2}\,s^{-1}}$ to mimic winter conditions in the field.

2.3 Lighting intensity experiment

To investigate the effect of light intensity on the growth of the strain KWT 167, batch culture experiments were performed using six different light-intensity treatments (20, 50, 100, 200, 350, and 500 $\mu\mathrm{mol\,m^{-2}\,s^{-1}}$) at 20°C. Light intensity was measured using Quantum Scalar Laboratory (QSL) radiometers (QSL-101, Biospherical Instruments Inc., San Diego, USA). Cells in the exponential growth phase that were cultured under 200 $\mu\mathrm{mol\,m^{-2}\,s^{-1}}$ were inoculated into 50 mL of fresh medium to achieve initial cell densities of approximately 100 cells mL^{-1} in each flask. The experiment was performed in triplicate at each light intensity until a decline in cell density was observed after reaching the maximum cell density.

2.4 Measurements of growth rate

Cells were counted every 2 days at the beginning of the experiment, but the frequency was reduced after cell growth reached the stationary phase. To count the cell numbers, a 2 mL sample from each flask was fixed with glutaraldehyde to a final concentration of 1%. More than 100 cells were counted for each sample, using a cytometer (Matsunami, Osaka, Japan) under an inverted light microscope (IX71, Olympus, Tokyo, Japan). The slope (S, day^{-1}) of the growth curve was calculated using four consecutive points and the following equation:

$$S=\frac{\ln N(t_2)-\ln N(t_1)}{t_2-t_1}$$

where N is the cell density (cells mL^{-1}) and t is the time (day). The value of the slope of day 2–8 in which cells were in early exponential phase was used to calculate the specific growth rate (μ, day^{-1}). In the temperature experiment, μ was subjected to linear regression analysis to derive the lower temperature limit (LTL) and the upper temperature limit (UTL), which correspond to growth rates of zero. The temperature at which the specific growth rate reached its maximum was defined as the optimum temperature (OT).

In the light intensity experiment, the maximum specific growth rate ($\mu_{\max}$) and the compensation light intensity (I_0) were estimated by fitting a double exponential decay function (Platt et al. 1980). The saturated light intensity (SL), at which μ equals the value of $\mu_{\max}$, was also calculated from the function. To address the limitation that the specific growth rate becomes 0 in the absence of light, the function was adapted for this study by incorporating an intercept, as follows:

$$\mu=M\left(1-\exp\left(-\frac{a}{M}(I-I_0)\right)\right)\times\exp\left(-\frac{b}{M}(I-I_0)\right) \quad (3)$$

where I represents light intensity and I_0 is the x–intercept, indicating the compensation light intensity. M, a, and b are constants; M is the maximum photosynthetic output attainable in the absence of photoinhibition, a is the slope of the initial linear segment of the curve, and b represents the degree of photoinhibition, in accordance with Platt et al. (1980).

In addition, the half saturation constant K_s was obtained

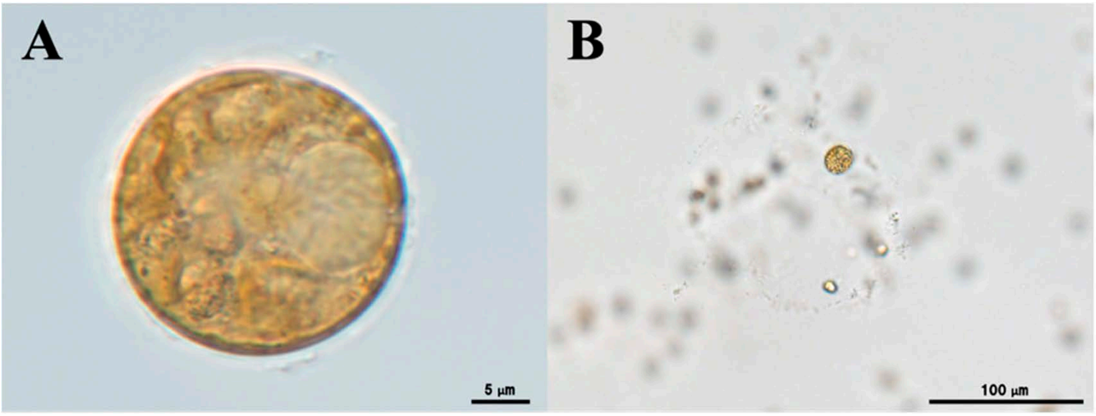

Fig. 1. *Prorocentrum* cf. *balticum* strain KWT167 observed under a light microscope. A) Whole cell; B) *P.* cf. *balticum* with mucosphere at 12 h after the start of co-cultivation with *Rhodomonas salina.*

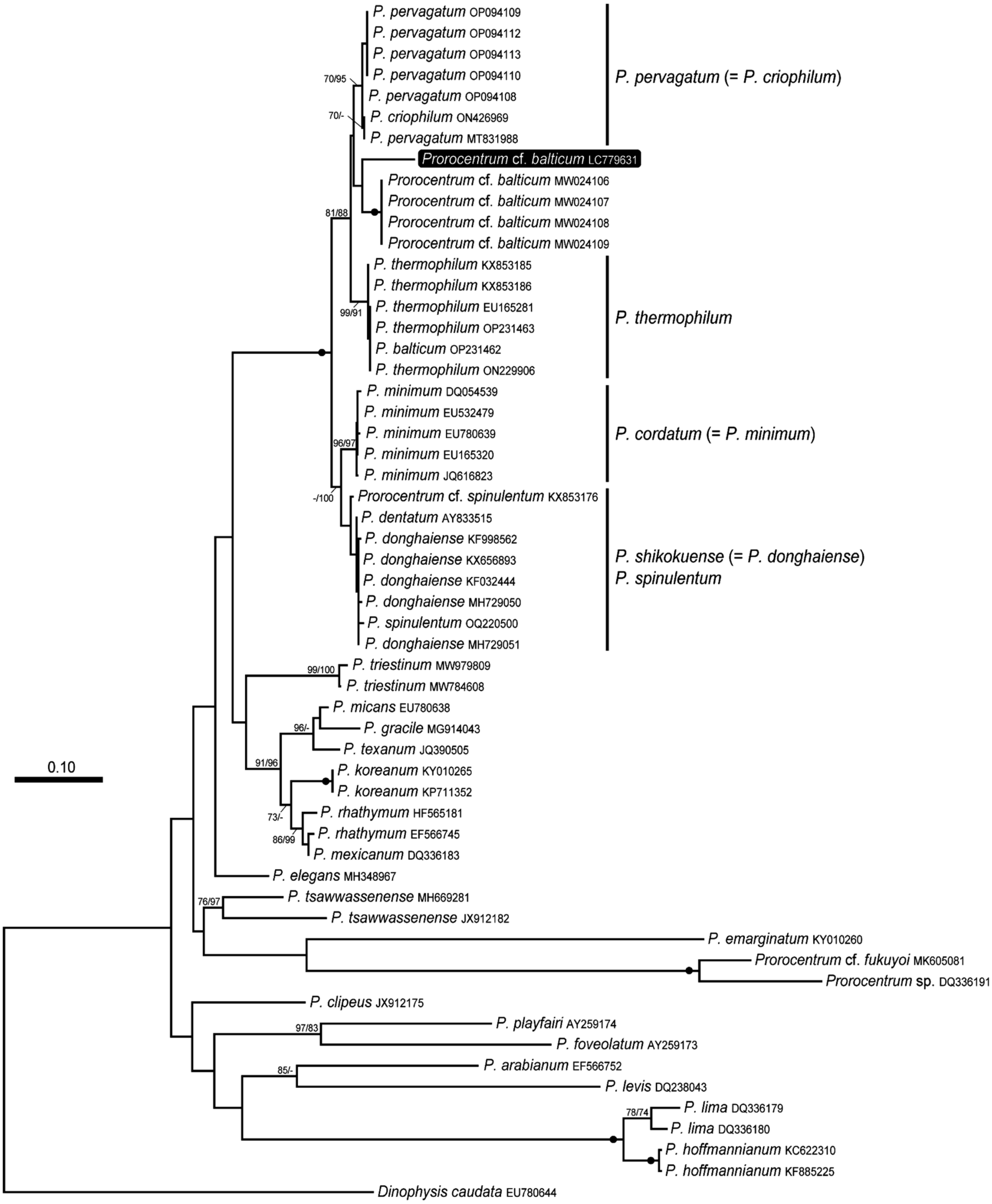

Fig. 2. Phylogenetic tree constructed based on the maximum likelihood (ML) method. LSU rDNA (D1–D3) sequences were aligned with sequences from GenBank. The strain used in this study is highlighted in the black box and it was closely related to *Prorocentrum* cf. *balticum* (MW024106–MW024109), which was described in Larsson et al. (2022). Black dots indicate maximum support (100%/100%). *Dinophysis caudata* (EU780644) was used as an outgroup.

by fitting the data in 20–350 μmol m^{-2} s^{-1} to a Michaelis–Menten equation with an adjusted intercept:

$$\mu = M' \frac{I - i_0}{K_S + I - 2i_0} \qquad (4)$$

where I is light intensity, and M', K_s and i_0 are constants: M' is the maximum photosynthetic output attainable in the absence of photoinhibition, K_s is the half saturation constant, and i_0 is the compensation light intensity. The competition coefficient α, defined as M'/K_s was also calculated.

2.5 Potential habitat estimation

The potential habitat of the strain KWT167, within the surface mixed layer was estimated using sea surface temperature (SST) and photosynthetically available radiation (PAR) across mid-latitudinal regions of the western North Pacific. A habitat conducive to growth was defined as areas where LTL≤SST≤UTL, and I is equal to or greater than the x–intercept I_0, based on the results of laboratory experiments. The monthly climatological SST and mixed layer depth between 120°E–165°E and 30°N–55°N were obtained from the Global Ocean Ensemble Physics Reanalysis (https://doi.org/10.48670/moi-00023) dataset for 1997 to 2022, and mean values were calculated. The mean PAR in the mixed layer was estimated based on the mixed layer depth, surface PAR, and the attenuation coefficient (K_d). The PAR and K_d data for the period 1997 to 2022 were obtained from the GlobColour website (https://hermes.acri.fr/). The spatial resolution was set as 0.1°×0.1°.

The future temperature and mixed layer depth under the RCP8.5 scenario were obtained from the FORP-NP10 version4 (Nishikawa et al. 2021) from the Data Integration and Analysis System (https://doi.org/10.20783/DIAS.655). We used the data of monthly temperature variations in 2100 under the RCP8.5 scenario. The mixed layered depth, 0.5°C lower than the surface temperature, was calculated based on the vertical temperature profiles. As for PAR and K_d data, the same data set was obtained for the period 1997 to 2022. The spatial resolution was 0.1°×0.1°.

2.6 Statistical analysis

An analysis of variance (ANOVA) and Tukey's HSD test were performed to determine the effects of temperature and light intensity on cell densities and the growth rates. All statistical analyses were conducted using R (R Core Team 2023).

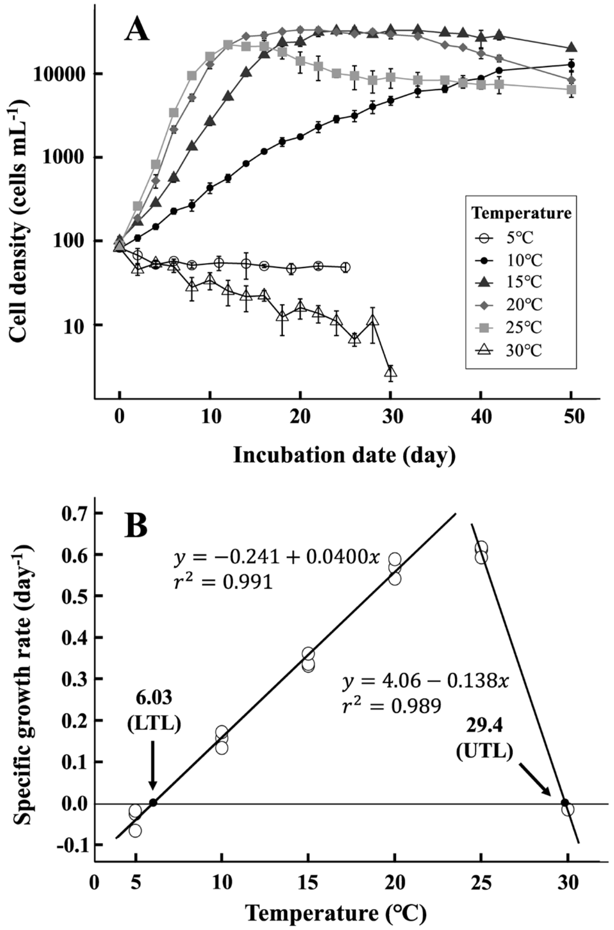

Fig. 3. Growth characteristics of *Prorocentrum* cf. *balticum* at various temperatures in batch culture. A) Temporal change of cell density. Light intensity was 200 μmol m^{-2} s^{-1} except for the 5°C treatment when 100 μmol m^{-2} s^{-1} was applied. Error bars show standard deviations. B) Specific growth rate as a function of temperature calculated from A). The lines are regression lines based on the data for 5–20°C and 25–30°C. Upper and lower temperature thresholds are also shown as ULT and LTL, respectively.

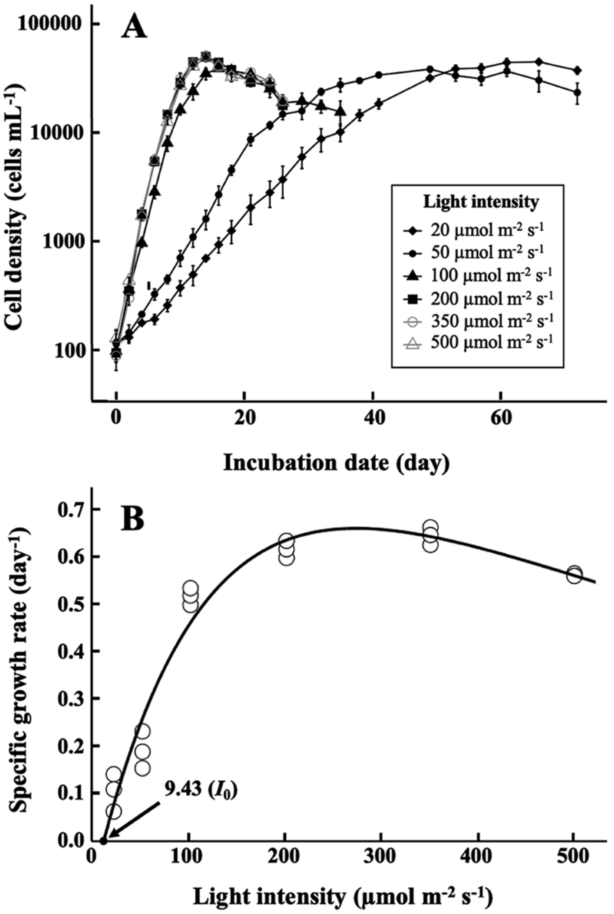

Fig. 4. Growth characteristics of *Prorocentrum* cf. *balticum* at different light intensities in batch culture at 20°C. Error bars show standard deviations. A) Temporal change in cell density. B) Specific growth rate as a function of light intensity calculated in A) by fitting using a double exponential decay function. Error bars show standard deviations. Compensation light intensity I_0=9.43 μmol m^{-2} s^{-1}, calculated from the regression, is also shown.

3. Results

3.1 Morphological and genetical characteristics

Cells of the strain KWT167 were round and measured $25\pm1.5\,\mu$m (n=30) in diameter (Fig. 1a), which resembled those of *Prorocentrum* cf. *balticum* from Australia except for the cell size ($\sim$15 μm, Larsson et al. 2022). Formation of a mucosphere was also confirmed in co-culture with *Rhodomonas salina* (Fig. 1b). In LSU rDNA phylogeny, strain KWT167 (LC779631) was closely related to the clade of *P.* cf. *balticum* from Australia, and then the roundish species *P. pervagatum* (=*Prorocentrum criophilum* Gourvil & Gutiérrez-Rodríguez) and *P. thermophilum* (Fig. 2). In the clade of spiny-surfaced *Prorocentrum*, strain KWT167 was distant from the clades of heart-shaped species *P. cordatum* and oblong species *Prorocentrum shikokuense* Hada, the latter has been reported also as *Prorocentrum donghaiense* Lu and *Prorocentrum obtusidens* Schiller (Shin et al. 2019). *Prorocentrum spinulentum* Tillmann, Gottschling & Hoppenrath was positioned within the clade of *P. shikokuense*. Based on this phylogenetic position, hereafter the strain KWT167 is referred to as *P.* cf. *balticum*.

3.2 Effect of temperature on growth

Prorocentrum cf. *balticum* showed substantial growth at temperatures between 10°C–25°C, but it did not grow at 30°C and 5°C (Fig. 3). At 15°C–25°C, cells of *P.* cf. *balticum* entered the exponential growth phase from day 2–4 and reached maximum densities of $\sim 3\times10^4$ cells mL^{-1} between day 12 and day 24. Subsequently, the cells entered stationary phases on days 12, 14, and 22 at 25°C, 20°C, and 15°C, respectively. At 10°C, the cell density increased exponentially from day 2 to day 50, but growth slowed at around day 25 when the maximum cell density was $\leq 10^4$ cells mL^{-1} (Fig. 3A). The cell density at 30°C decreased from day 2 and no living cells were observed at day 32. The density of cells maintained at 5°C under 100 μmol m^{-2} s^{-1} decreased from 100 cells mL^{-1} on day 0 to approximately 50 cells mL^{-1} on day 4, before remaining constant until the end of the experiment on day 24.

Specific growth rates increased with temperature over the range of 10°C to 25°C (Fig. 3B). Although the growth rate at the OT of 25°C was the highest at 0.609 ± 0.010 day^{-1} (Table S1A), it was not significantly different from that at 20°C (0.568 ± 0.019 day^{-1}) (ANOVA with Tukey's HSD test, $p>0.05$). Extrapolation of the regression line with data from 5°C to 20°C indicated that the LTL, at

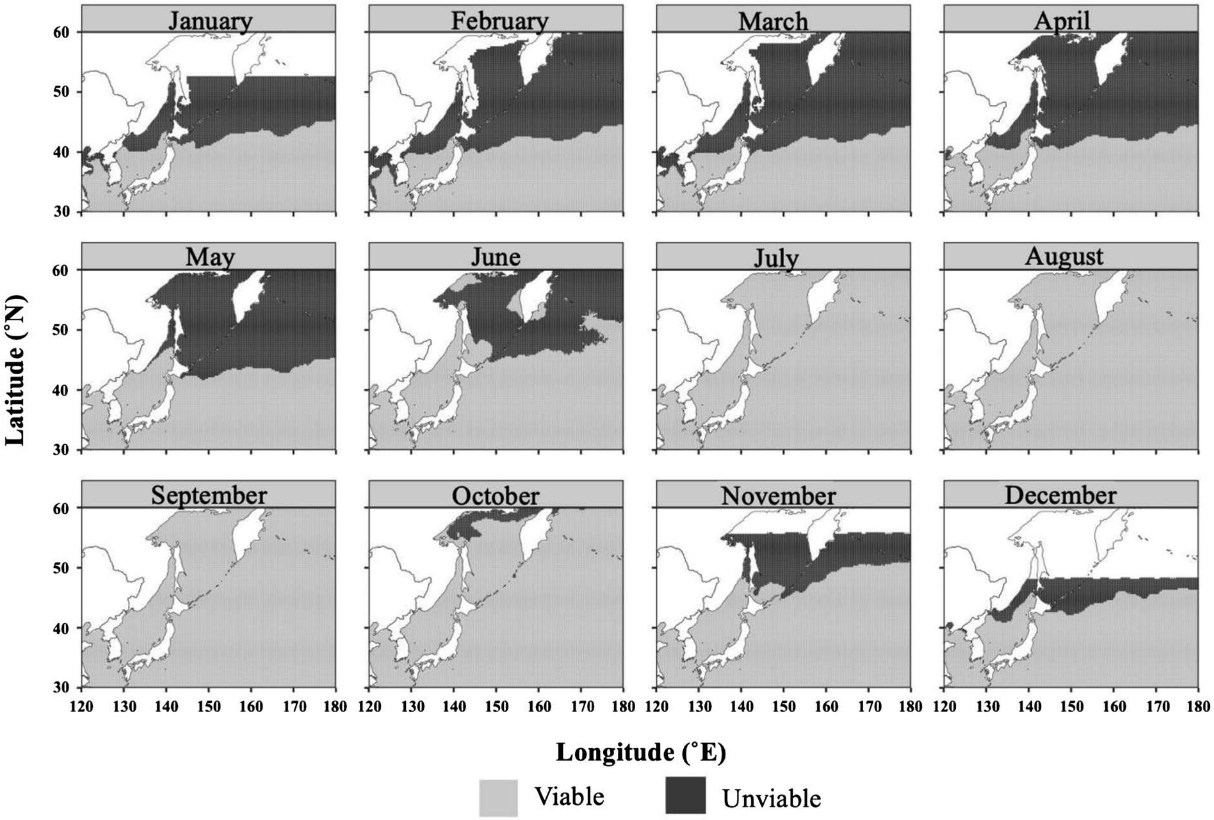

Fig. 5. Monthly variations in the potential habitat of *Prorocentrum* cf. *balticum* around Japan estimated based on LTL, UTL, and I_0 data derived from the incubation experiments. The light grey area (viable) shows the area that fulfils the conditions for growth, and the dark grey area (unviable) shows the area that does not. No data is available for the white area. The datasets for sea surface temperature and the light intensity of the mixed layer were obtained from the Global Ocean Ensemble Physics Reanalysis dataset (the average from 1997 to 2020).

which there was no growth, was 6.03°C. The UTL, which was also estimated using the regression line between 25°C and 30°C, was 29.4°C (Fig. 3B).

3.3 Effect of light intensity on growth

Cell densities increased exponentially and reached maximum levels of $\sim 5\times10^4$ cells mL^{-1} at all light intensities (i.e., 20 to 500 $\mu mol\ m^{-2}\ s^{-1}$). Under higher light intensities ($\geq 100\ \mu mol\ m^{-2}\ s^{-1}$), cell densities peaked at days 14–16 before decreasing (Fig. 4A). Above 200 $\mu mol\ m^{-2}\ s^{-1}$, no significant differences were observed in cell densities after day 4 (ANOVA with Tukey's HSD test, $p>0.05$), however, cell densities at 100 $\mu mol\ m^{-2}\ s^{-1}$ were significantly different from those at 200–500 $\mu mol\ m^{-2}\ s^{-1}$ from day 4 to day 14 ($p<0.05$). Under low light intensities (20 and 50 $\mu mol\ m^{-2}\ s^{-1}$), growth was slower than that at higher light intensities, with cell densities peaking at day 49 and day 66, respectively, followed by a stationary growth phase for ≥10 days. Growth was observed during day 0–6 at higher light intensities (100–500 $\mu mol\ m^{-2}\ s^{-1}$), followed by 20 $\mu mol\ m^{-2}\ s^{-1}$ (day 8–14) and 50 $\mu mol\ m^{-2}\ s^{-1}$ (day 14–21) (Table S1B).

The specific growth rate at different light intensities increased from 20 $\mu mol\ m^{-2}\ s^{-1}$ (0.105 ± 0.032 day^{-1}) to 350 $\mu mol\ m^{-2}\ s^{-1}$ (0.645 ± 0.015 day^{-1}) and decreased at 500 $\mu mol\ m^{-2}\ s^{-1}$ (0.562 ± 0.002 day^{-1}) (Fig. 4B, Table S1B). No significant difference in specific growth rates was observed between 200 $\mu mol\ m^{-2}\ s^{-1}$ (0.616 ± 0.015 day^{-1}) and 350 $\mu mol\ m^{-2}\ s^{-1}$ (0.645 ± 0.015 day^{-1}) (ANOVA with Tukey's HSD test, $p>0.05$), while the specific growth rate at 500 $\mu mol\ m^{-2}\ s^{-1}$ was significantly lower than that at 350 $\mu mol\ m^{-2}\ s^{-1}$ ($p<0.05$). The compensation light intensity, I_0, obtained from Eq. (3) was 9.43 $\mu mol\ m^{-2}\ s^{-1}$ (Fig. 4B). The maximum specific growth rate, μ_{max}, and SL calculated from the regression curve were 0.661 day^{-1} and 273 $\mu mol\ m^{-2}\ s^{-1}$, respectively (Fig. 4B). K_s and α obtained from Michaelis–Menten equation (Eq. (4)) were 86.8 $\mu mol\ m^{-2}\ s^{-1}$ and 0.00954, respectively.

3.4 Potential habitat estimation

The habitats conducive to positive growth of *Prorocentrum* cf. *balticum* (referred to as viable habitats hereafter) were defined as areas where the SST ranges between 6.03°C (LTL) and 29.4°C (UTL), and the light intensity is $\geq 9.43\ \mu mol\ m^{-2}\ s^{-1}$ (I_0). Our results showed that the boundary between viable and unviable areas for the growth of *P.* cf. *balticum*, in terms of temperature and light intensity, was located at around 40°N–42°N from December to June (Fig. 5). However, from July to November, conditions that were conducive to substantial growth were

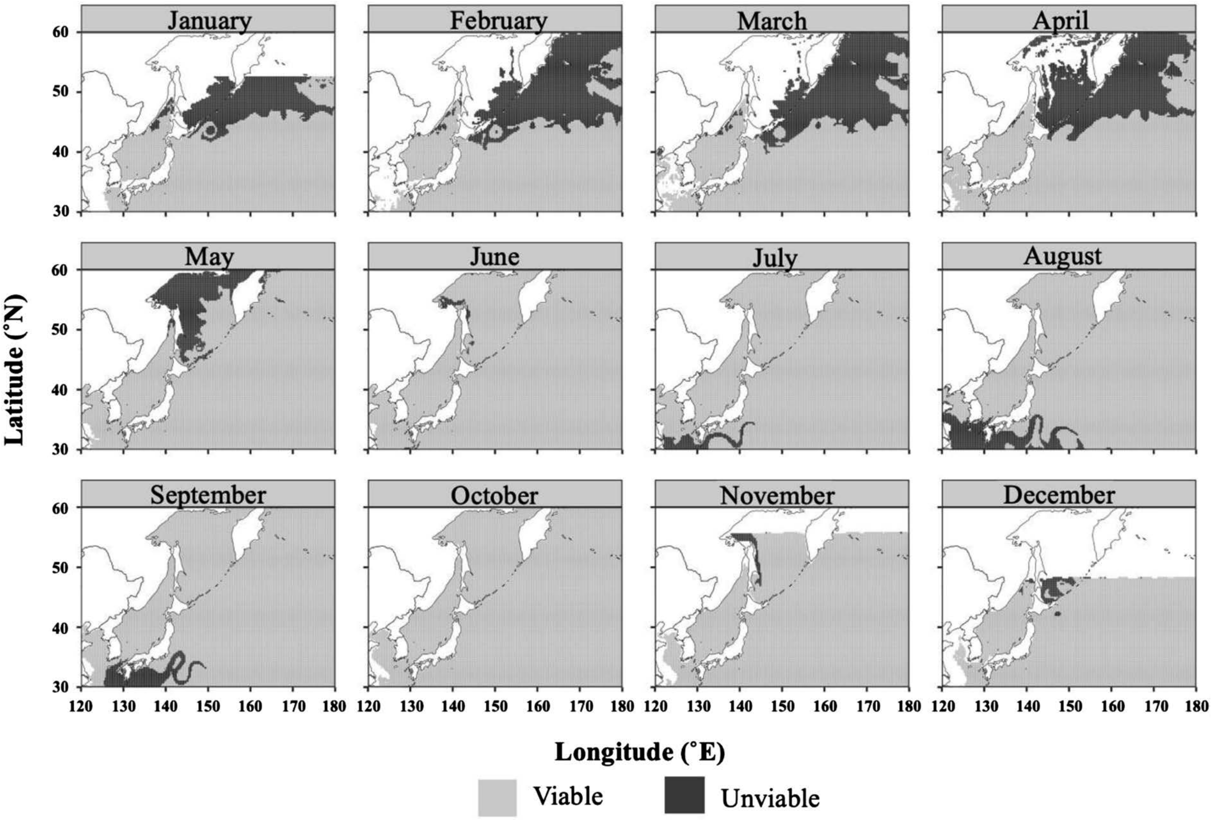

Fig. 6. Future-predicted monthly variations of *Prorocentrum* cf. *balticum* around Japan estimated based on LTL, UTL, and I_0 derived from the incubation experiments. The light grey area (viable) shows the area that fulfils the conditions for growth, and the dark grey area (unviable) shows the area that does not. The temperature and mixed layer depth under the RCP8.5 scenario in 2100 were obtained from the FORP-NP10 version4. The dataset for light intensity used to calculate the mixed layer average light intensity was the same as that used in Fig. 3.

observed across all areas around Japan (Fig. 5). Within the mixed layer, no constraints due to light intensity were detected throughout the year. Regarding future projections of potential habitat under the RCP8.5 scenario, which assumes that CO_2 emissions will continue to rise throughout the 21st century, the habitable zone for *P.* cf. *balticum* is predicted to expand to include almost all of the ocean areas around Japan throughout the year except for the coastal waters of eastern Hokkaido during the winter time (Fig. 6). On the other hand, unviable habitats occurred in the southern part of Japan from July to September due to high temperature.

4. Discussion

The spiny-surfaced planktonic *Prorocentrum* isolated from off the Pacific coast of northeastern Japan, the strain KWT167, could be identified as *Prorocentrum* cf. *balticum* based on the phylogenetic position (Fig. 2). On the other hand, for comparison of its ecophysiological traits, molecular identification is unavailable for *P. balticum* in occurrence reports and strains used for growth experiments in previous studies. Therefore, morphologically-identified nominal *P. balticum* in previous studies may include other related species with a close morphological resemblance, such as *P. pervagatum* and *P. thermophilum*.

The findings of this study showed that *Prorocentrum* cf. *balticum* is adapted to a wide range of temperatures, from 6°C to 29°C. To date, the occurrence of morphologically-identified nominal *P. balticum* has been reported from across the world's oceans, ranging from the Arctic to tropical waters (Table 1). The findings of this study are generally in agreement with the documented occurrence patterns of morphologically-identified nominal *P. balticum*, with two notable exceptions: the presence of the species at the highest latitudes in the Chukuchi Sea in September (Yokoi et al. 2015), where the temperature fell below the LTL for our strain, and the lowest latitudes of the Caribbean in December (Salon-Barros et al. 2016), where the temperature exceeded the UTL. These discrepancies suggest that the *P. balticum* in the Chukuchi Sea and Caribbean might have been misidentified, or they may possess adaptations to temperatures outside the range identified for our strain. Recently described species, *P. thermophilum* and *P. pervagatum*, which are genetically closely related to *P.* cf. *balticum*, were found from tropical and boreal waters, respectively (Gómez et al. 2023, Tillmann et al. 2023c). This discovery supports the notion of potential habitat segregation among *Prorocentrum* species, suggesting that they may occupy distinct ecological niches based on tempera-

Table 1. Distribution of nominal *Prorocentrum balticum* (the small roundish *Prorocentrum* reported as *Prorocentrum balticum*) in previous studies.

Region	Latitude	Observed Year	Month	Temperature (°C)	Cell density (cells mL^{-1})	Reference
Gulf of Nicoya, Costa Rica	9–10°N	1985, 1986	May–Aug.	26–31	>1000	Vrquez & Hargraves 1995
Cartagena bay, Caribbean	10°N	2015	Dec.	30.2±0.12	3200–5400	Salon-Barros et al. 2016
Red Sea	14.5°N	2012–2013	—	—	0.28	Alkawri et al. 2016
Bahia de Mazatlan, Mexico	23°N	2000	May	18–26	>20000	Alonso-Rodriguez & Ochoa 2004
Gulf of California, Mexico	24°N	2012	Aug.	—	0.4	Gárate-Lizárraga 2013
Indian River Lagoon, the US	27–28°N	1997–1999	—	12–32	—	Badylak & Phlips 2004
Tampa Bay, the US	27–28°N	2002–2003	All year	13.3–31.4	—	Badylak et al. 2007
Changjiang Estuary	31°N	—	—	—	—	Lu & Goebel 2001
Jeju Island, Korea	33–34°N	2006–2016	—	—	—	Lee & Kim 2017
Jeju Island, Korea	33–34°N	2006–2009	Jun.–Sep.	—	—	Kim et al. 2013
Gamtoos Estuary, South Africa	33–34°S	2018	Jul.–Oct.	13–23	1699 (including *P. minimum*)	Lemley & Adams 2020
Mediterranean	35–36°N	2018	Oct.	—	—	Idmoussi et al. 2020
Elefsis Bay, Greece	38°N	1975, 1976	All year	10–26.1	—	Ignatiades 1984
Bay of Biscay, Spain	43–44°N	1987	Jul.	18–19	3.6	Botas et al. 1990
Subarctic Western North Pacific	43–44°N	1969	Mar.–May	—	3.3	Taylor & Waters 1982
Adriatic Sea	44–45°N	2006	May	17–18	>100	Ivančić et al. 2010
Black Sea	44–45°N	2020	Mar.–Jul.	9.2–25.6	—	Pospelova & Priimak 2021
Atlantic Ocean, Ireland	49–54°N	1995	Jun.–Jul.	9–12	—	Raine et al. 2002
Western English Channel	50.25°N	1997	Sep.–Oct.	14–18	3360	Widdicombe et al. 2010
Baltic Sea	54–55°N	1986–1990	—	16.9±3.3	>1000	Telesh et al. 2016
Baltic Sea	54–55°N	1906	May–Jun.	—	—	Wasmund et al. 2008
Baltic Sea	54–55°N	1972, 1973	May	—	—	Wasmund et al. 2008
Donegal Bay, Ireland	54–55°N	1997	Nov.	—	>16000	O'Boyle et al. 2001
White Sea	66.3°N	2002	Jul.–Sep.	6°C-16	—	Vershinin et al. 2006
Chukchi Sea	72.5°N	2013	Sep.	−1.5–3.3	0.2	Yokoi et al. 2015

ture preferences. On the other hand, temperature adaptations have also been observed in other dinoflagellates, e.g., *Alexandrium catenella* (Whedon & Kofoid) Balech, *Alexandrium ostenfeldii* (Paulsen) Balech & Tangen and *Margalefidinium polykrikoides* (Margalef) F.Gómez, Richlen & D.M.Anderson, where isolates from different geographical locations exhibited different growth temperature ranges (Kim et al. 2004, Laabir et al. 2011, Kudela & Gobler 2012, Lim et al. 2019). Since we have only used a single strain to examine the growth characteristics of *P.* cf. *balticum*, further investigation is required with a variation of ecotypes (or ribotypes) to determine the physiological characteristics of this species.

The maximum specific growth rate for *P.* cf. *balticum* (0.661 day^{-1}) was comparable to other bloom-forming *Prorocentrum*, including genetically closely related species such as *P. shikokuense* (reported as *P. donghaiense*) and *P. cordatum* (as *P. minimum*) (Table 2, Fig. 2). This suggests that the strain used in this study has the potential to form blooms under favorable environmental conditions. The OT for *P.* cf. *balticum* (25°C under 200 $\mu\text{mol m}^{-2}\,\text{s}^{-1}$) was similar to those observed in other genetically related *Prorocentrum* species (Table 2). However, the UTL for *P.* cf. *balticum* (29°C) was lower than that observed for *P. shikokuense* (31°C; Xu et al. 2010) and *P. cordatum* (31°C; Grzebyk & Berland 1996). Furthermore, the LTL for *P.* cf. *balticum* (6°C) was markedly lower than that in *P. shikokuense* (<10°C; Xu et al. 2010) and *P. cordatum* (13°C; Grzebyk & Berland 1996) as well as most other *Prorocentrum* species (Table 2). These results suggest that *P.* cf. *balticum* is adapted to a broader range of lower temperatures than other *Prorocentrum* species. For example, Telesh et al. (2016) reported high abundances of nominal *P. balticum* at lower temperatures (16.9±3.3°C) compared to those favorable for *P. cordatum* (reported as *P. minimum*) (20.8±3.7°C) in the Baltic Sea.

As for the light environment, the SL at which the highest growth rate in *P.* cf. *balticum* was observed (273 $\mu\text{mol m}^{-2}\,\text{s}^{-1}$) was the highest among previously studied *Prorocentrum* species, including *P. shikokuense* (reported as *P. donghaiense*), *Prorocentrum micans* Ehrenberg, and *P. cordatum* (as *P. minimum*) (Table 3). This comparison with previous studies also reveals that *P.* cf. *balticum* has the highest K_s (86.8 $\mu\text{mol m}^{-2}\,\text{s}^{-1}$)

Table 2. Growth characteristics of *Prorocentrum* reported in previous studies compared with the results of this study. LTL and UTL are the lower and upper limits of the temperature for growth, respectively. OT is the optimum temperature at which the specific growth rate is the highest. μmax is the maximum specific growth rate.

Species	Sampling place	LTL	UTL	OT	μmax	Reference
Prorocentrum belizeanum	—	—	—	25	0.204	López-Rosales et al. 2014
Prorocentrum donghaiense	—	—	—	20	0.23	Shen et al. 2016
Prorocentrum mexicanum	Knight Key, Florida	23	33	27	0.25	Morton et al. 1992
Prorocentrum concavum	Knight Key, Florida	21	31	27	0.28	Morton et al. 1992
Prorocentrum lima	Knight Key, Florida	21	33	27	0.29	Morton et al. 1992
Prorocentrum micans	Muroran harbor, Japan	5	—	20	0.39	Uchida 1981
Prorocentrum hoffmannianum	St. John, US Virgin Islands	<22	>31	27	0.53	Morton et al. 1994
Prorocentrum rhathymum	Kadan Island, Myanmar	<15	>30	25	0.62	Su-Myat & Koike 2013
Prorocentrum donghaiense	Zhoushan, China	—	—	25–30	0.65	Hu et al. 2016
Prorocentrum cf. *balticum*	North Pacific, Japan	6.03	29.4	25	0.661	This study
Prorocentrum donghaiense	East China Sea	<10	31	27	0.77	Xu et al. 2010
Prorocentrum shikokuense	Kadan Island, Myanmar	<15	>30	15	0.87	Su-Myat & Koike 2013
Prorocentrum minimum	—	<5	>23	—	0.88	Trick et al. 1984
Prorocentrum triestinum	Seto Inland Sea, Japan	<10	>30	20	0.95	Nishijima et al. 1989
Prorocentrum minimum	Mediterranean	13	31	26.5	1.13	Grzebyk & Berland 1996

Table 3. Values for compensation light intensity (I_0), half saturation constant (Ks), competition coefficient (α), and saturation light intensity (SL) obtained for *Prorocentrum* species obtained in previous studies compared with those obtained in this study. * Indicates that I_0, Ks, and α were calculated using equation (4), as these parameters were not specified in the original literature.

Species	I_0	Ks	α	SL	Reference
Prorocentrum cf. *balticum*	9.43	86.8	0.00954	273	This study
Prorocentrum donghaiense	0.1	2.61	0.26	30	Xu et al. 2010
Prorocentrum donghaiense	4.7	78.0	0.0179	>200	Hu et al. 2016
Prorocentrum micans	6.12*	13.9*	0.0419*	>90	Uchida 1981
Prorocentrum minimum	4.49*	26.1*	0.0356*	90	Trick et al. 1984

among these *Prorocentrum* species. Moreover, the I_0 (9.43 μmol m^{-2} s^{-1}) was the highest and the α (0.00954) was the lowest among the species compared (Table 3). All this finding suggests that *P.* cf. *balticum* is well-adapted to environments with high light intensity. The I_0 for *P.* cf. *balticum* was low enough to maintain its population around Japan throughout the years.

Overall, the findings of this study showed that the growth characteristics of *P.* cf. *balticum* are relatively eurythermal and generally adapted to high light intensity environments, such as subtropical waters and mid-latitudinal areas during summer. Accordingly, the analysis estimating the potential distribution area suggested that the northern limit of *P.* cf. *balticum* distribution extends to approximately 40°N–42°N during the summer months. This is largely consistent with the cosmopolitan distribution pattern for *P.* cf. *balticum* in the world's subtropical oceans as reported by Larsson et al. (2022), although this result from *Tara Oceans* data set may include other related *Prorocentrum* possessing the identical SSU rDNA (V9) sequences (129 bp) to that of *P.* cf. *balticum*, such as *P. cordatum*, *P. pervagatum*, *P. thermophilum*, *P. shikokuense*, and *P. spinulentum*. A cosmopolitan distribution pattern also would imply that nutrient depletion due to stratification in subtropical environments would not be a constraint on the growth of *P.* cf. *balticum*, as it is mixotrophic, utilizing mechanisms such as mucus traps (Larsson et al. 2022). It has been reported that the mixotrophic *Prorocentrum* species, *P. cordatum* and *P. pervagtum* also use mucus traps, and *P. pervagatum* has higher growth rates when provided with food compared to non-fed control cultures (Tillmann et al. 2023b). Another important feature of *P.* cf. *balticum* is its tolerance to low temperatures compared to other *Prorocentrum* species, suggesting that it could overwinter in areas at the periphery of its distribution range and then commence rapid growth as temperatures rise in spring. Consequently, as shown in this study, *P.* cf. *balticum* has a high potential to extend its range northward in response to future global warming. This potential for expansion may have profound implications for biogeochemical cycles and food web structure in the Oyashio region, a strong sink for atmospheric CO_2 (Midorikawa et al. 2003) and an important fishing ground (Sakurai 2007). The adaptability of *P.* cf. *balticum* to the potentially expanding subtropical environments, coupled with its mixotrophic feeding behavior using a mucus trap, could potentially enhance carbon fluxes (Larsson et al. 2022). To fully elucidate the impact of *P.* cf. *balticum* within marine ecosystems, further investigations into its physiological and ecological responses to environmental variables, including salinity and nutrient availability, as well as its prey-predatory relationships and mixotrophic feeding habits, are considered necessary.

Electronic supplementary material.

The online version of this article (doi: 10.3800/pbr.19.191) contains supplementary material: Table S1. Growth rate, μ, and its standard deviation for *Prorocentrum* cf. *balticum* grown in a batch culture under A) various temperatures in 100 μmol m^{-2} s^{-1} for 5°C and 200 μmol m^{-2} s^{-1} for others, and B) various light intensities at 20°C.

Acknowledgements

We are grateful to the captain, crew, and researchers aboard the *R/V Wakataka-maru* for their cooperation with the sample collection during cruise WK2207. The present study was funded by a Grant-in-Aid for Scientific Research (B) (16H04959 and 20H03059) and (S) (24H00075) from the Ministry of Education, Science, Sports, and Culture.

References

Alkawri A, Abker M, Qutaei E, Alhag M, Qutaei N, Mahdy S (2016) The first recorded bloom of *Pyrodinium bahamense* var. *bahamense* Plate in Yemeni coastal waters off Red Sea, near Al Hodeida City. Turkish J Fish Aquat Sci 16: 275–282.

Alonso-Rodrıguez R, Ochoa JL (2004) Hydrology of winter–spring "red tides" in Bahía de Mazatlán, Sinaloa, México. Harmful Algae 3: 163–171.

Badylak S, Phlips EJ (2004) Spatial and temporal patterns of phytoplankton composition in subtropical coastal lagoon, the Indian River Lagoon, Florida, USA. J Plankton Res 26: 1229–1247.

Badylak S, Phlips EJ, Baker P, Fajans J, Boler R (2007) Distributions of phytoplankton in Tampa Bay Estuary, U.S.A. 2002–2003. Bull Mar Sci 80: 295–317.

Botas JA, Fernandez E, Bode A, Anadon R (1990) A persistent upwelling off the Central Cantabrian Coast (Bay of Biscay). Estuar Coast Shelf Sci 30: 185–199.

Faust MA, Moestrup Ø, Larsen J (1999) Potentially toxic phytoplankton (3) *Prorocentrum* (Dinophyceae). ICES Identification Leaflets for Plankton 184: 1–24.

Gárate-Lizárraga I (2013) Bloom of *Cochlodinium polykrikoides* (Dinophyceae: Gymnodiniales) in Bahía de La Paz, Gulf of California. Mar Pollut Bull 67: 217–222.

Glibert PM, Burkholder JM, Kana TM (2012) Recent insights about relationships between nutrient availability, forms, and stoichiometry, and the distribution, ecophysiology, and food web effects of pelagic and benthic *Prorocentrum* species. Harmful Algae 14: 231–259.

Gómez F, Zhang H, Roselli L, Lin S (2022) Detection of *Prorocentrum shikokuense* in the Mediterranean Sea and evidence that *P. dentatum*, *P. obtusidens* and *P. shikokuense* are three different species (Prorocentrales, Dinophyceae). ACTA Protozool 60: 47–59.

Gómez F, Gourvil P, Li T, Huang Y, Zhang H, Courcot L, Artigas LF, Soler Onís ES, Gutiérrez-Rodríguez A, Lin S (2023) Molecular phylogeny of the spiny-surfaced species of the dinoflagellate *Prorocentrum* with the description of *P. thermophilum* sp. nov. and *P. criophilum* sp. nov. (Prorocentrales, Dinophyceae). J Phycol 59: 70–86.

Grzebyk D, Berland B (1996) Influences of temperature, salinity and irradiance on growth of *Prorocentrum minimum* (Dinophyceae) from the Mediterranean Sea. J Plankton Res 18: 1837–1849.

Hartmann M, Grob C, Tarran GA, Martin AP, Burkill PH, Scanlan DJ, Zubkov MV (2012) Mixotrophic basis of Atlantic oligotrophic ecosystems. Proc Natl Acad Sci USA 109: 5756–5760.

Heil CA, Glibert PM, Fan C (2005) *Prorocentrum minimum* (Pavillard) Schiller: A review of a harmful algal bloom species of growing worldwide importance. Harmful Algae 4: 449–470.

Hu Z, Mulholland MR, Xu N, Duan S (2016) Effects of temperature, irradiance and $p\mathrm{CO}_2$ on the growth and nitrogen utilization of *Prorocentrum donghaiense*. Aquat Microb Ecol 77: 155–166.

Ianora A, Poulet SA, Miralto A (2003) The effects of diatoms on copepod reproduction: A review. Phycologia 42: 351–363.

Idmoussi H, Somoue L, Hilmi K, Ettahiri O, Baibai T, Makaoui A, Errhif A (2020) Phytoplankton assemblage characterization along the Mediterranean coast of Morocco during autumn. Firenze University Press Best Practice in Scholarly Publishing: 547–556.

Ignatiades L (1984) Coarse-scale horizontal distribution of phytoplankton in a semi-enclosed coastal area. Mar Ecol 5: 217–227.

Ivančić I, Fuks D, Radić T, Lyons DM, Šilović T, Kraus R, Precali R (2010) Phytoplankton and bacterial alkaline phosphatase activity in the northern Adriatic Sea. Mar Environ Res 69: 85–94.

Kim D, Matsuyama Y, Nagasoe S, Yamaguchi M, Yoon Y, Oshima Y, Imada N, Honjo T (2004) Effects of temperature, salinity and irradiance on the growth of the harmful red tide dinoflagellate *Cochlodinium polykrikoides* Margalef (Dinophyceae). J Plankton Res 26: 61–66.

Kim HS, Kim SH, Jung MM, Lee JB (2013) New record of dinoflagellates around Jeju Island. J Ecol Environ 36: 273–291.

Kudela RM, Gobler CJ (2012) Harmful dinoflagellate blooms caused by *Cochlodinium* sp.: Global expansion and ecological strategies facilitating bloom formation. Harmful Algae 14: 71–86.

Kuwata K, Lum WM, Takahashi K, Benico G, Uchida H, Ozawa R, Matsushima R, Watanabe H, Oikawa T, Suzuki T, Iwataki M (2023) A new small thecate dinoflagellate *Azadinium anteroporum* sp. nov. (Amphidomataceae, Dinophyceae) isolated from the Asian Pacific. Phycologia 62: 303–314.

Laabir M, Jauzein C, Genovesi B, Masseret E, Grzebyk D, Cecchi P, Vaquer A, Perrin Y, Collos Y (2011) Influence of temperature, salinity and irradiance on the growth and cell yield of the harmful red tide dinoflagellate *Alexandrium catenella* colonizing Mediterranean waters. J Plankton Res 33: 1550–1563.

Larsson ME, Bramucci AR, Collins S, Hallegraeff G, Kahlke T, Raina J, Seymour JR, Doblin MA (2022) Mucospheres produced by a mixotrophic protist impact ocean carbon cycling. Nat Commun 13: 1301.

Lee JB, Kim GB (2017) New records of two genera *Mesoporos* and *Prorocentrum* (Prorocentraceae, Prorocentrales, Dinophyceae) in Korean waters. Korean J Environ Biol 35: 265–272.

Lee T, Fong F, Ho KC, Lee F (2016) The mechanism of diarrhetic shellfish poisoning toxin production in *Prorocentrum* spp.: Physiological and molecular perspectives. Toxins 8: 272.

Lemley DA, Adams JB (2020) Physico-chemical and microalgal gradients change rapidly in response to mouth closure in a predominantly open estuary. Afr J Aquat Sci 45: 11–21.

Lim AS, Jeong HJ, Ok JH, You JH, Kang HC, Kim SJ (2019) Effects of light intensity and temperature on growth and ingestion rates of the mixotrophic dinoflagellate *Alexandrium pohangense*. Mar Biol 166: 1–11.

Lohmann H (1908) Untersuchungen zur Feststellung des vollständigen Gehaltes des Meeres an Plankton. Wissenschaftliche Meeresuntersuchungen, Abteilung Kiel, Neue Folge 10: 129–370.

López-Rosales L, Gallardo-Rodríguez J, Sánchez-Mirón A, Cerón-García M, Belarbi E, García-Camacho F, Molina-Grima E (2014) Simultaneous effect of temperature and irradiance on growth and okadaic acid production from the marine dinoflagellate *Prorocentrum belizeanum*. Toxins 6: 229–253.

Lu D, Goebel J (2001) Five red tide species in genus *Prorocentrum* including the description of *Prorocentrum donghaiense* Lu SP. nov. from the East China Sea. Chin J Oceanol 19: 337–344.

Lu S, Ou L, Dai X, Cui L, Dong Y, Wang P, Li D, Lu D (2022) An overview of *Prorocentrum donghaiense* blooms in China: Species identification, occurrences, ecological consequences, and factors regulating prevalence. Harmful Algae 114: 102207.

Midorikawa T, Iwano S, Saito K, Takano H, Kamiya H, Ishii M, Inoue HY (2003) Seasonal changes in oceanic $p\mathrm{CO}_2$ in the Oyashio region from winter to spring. J Oceanogr 59: 871–882.

Mitra A, Caron DA, Faure E, Flynn KJ, Leles SG, Hansen PJ, McManus GB, Not F, Gomes HR, Santoferrara LF, Stoecker DK, Tillmann U (2023) The mixoplankton database (MDB): Diversity of photo-phago-trophic plankton in form, function, and distribution across the global ocean. J Eukaryot Microbiol 70: e12972.

Morton SL, Norris DR, Bomber JW (1992) Effect of temperature, salinity and light intensity on the growth and seasonality of toxic dinoflagellates associated with ciguatera. J Exp Mar Biol Ecol 157: 79–90.

Morton SL, Bomber JW, Tindall PM (1994) Environmental-effects on the production of okadaic acid from *Prorocentrum hoffmannianum* Faust I. temperature, light, and salinity. J Exp Mar Biol Ecol 178: 67–77.

Nishikawa S, Wakamatsu T, Ishizaki H, Sakamoto K, Tanaka Y, Tsujino H, Yamanaka G, Kamachi K, Ishikawa Y (2021) Development of high-resolution future ocean regional projection datasets for coastal applications in Japan. Prog Earth Planet Sci 8: 7.

Nishijima T, Hata Y, Yamauchi S (1989) Physiological ecology of *Prorocentrum triestinum*. Nippon Suisan Gakkaishi 55: 2009–2014.

O'Boyle S, Nolan G, Raine R (2001) Harmful phytoplankton events caused by variability in the Irish Coastal Current along the west of Ireland. In: *Harmful Algal Blooms 2000: Proceedings of the 9th International Conference on Harmful Algal Blooms* (eds Hallegraeff GM, Blackburn SI, Bolch CJ, Lewis RJ). UNESCO IOC, Hobart, Australia, pp. 145–149.

Platt T, Gallegos CL, Harrison WG (1980) Photoinhibition of photosynthesis in natural assemblages of marine phytoplankton. J Mar Res 38: 687–701.

Polovina JJ, Dunne JP, Woodworth PA, Howell EA (2011) Projected expansion of the subtropical biome and contraction of the temperate and equatorial upwelling biomes in the North Pacific under global warming. ICES J Mar Sci 68: 986–995.

Pospelova N, Priimak A (2021) The role of microalgae of the genus *Prorocentrum* in the diet of mussels *Mytilus galloprovincialis* (Lamarck, 1819) (Black Sea) in suspended culture. Environ Earth Sci 937: 022072.

R Core Team (2023) R: a language and environment for statistical computing, R Foundation for Statistical Computing [code]. Available at: https://www.R-project.org/ (accessed on 9 September 2023).

Raine R, White M, Dodge JD (2002) The summer distribution of net plankton dinoflagellates and their relation to water movements in the NE Atlantic Ocean, west of Ireland. J Plankton Res 24: 1131–1147.

Sakka A, Legendre L, Gosselin M, Delesalle B (2000) Structure of the oligotrophic planktonic food web under low grazing of heterotrophic bacteria: Takapoto Atoll, French Polynesia. Mar Ecol Prog Ser 197: 1–17.

Sakurai Y (2007) An overview of the Oyashio ecosystem. Deep Sea Res Part II Top Stud Oceanogr 54: 2526–2542.

Salon-Barros JC, Hoyos-Acuña JJ, Arregoces LJ, Mancera JE (2016) *Prorocentrum lima* and *Prorocentrum balticum* blooms in Cartagena de Indias, Colombian Caribbean. Harmful Algae News 53: 9.

Shen A, Ma Z, Jiang K, Li D (2016) Effects of temperature on growth, photophysiology, Rubisco gene expression in *Prorocentrum donghaiense* and *Karenia mikimotoi*. Ocean Sci J 51: 581–589.

Shin HH, Li Z, Mertens KN, Seo MH, Gu H, Lim WA, Yoon YH, Soh HY, Matsuoka K (2019) *Prorocentrum shikokuense* Hada and *P. donghaiense* Lu are junior synonyms of *P. obtusidens* Schiller, but not of *P. dentatum* Stein (Prorocentrales, Dinophyceae). Harmful Algae 89: 101686.

Stecher G, Tamura K, Kumar S (2020) Molecular Evolutionary Genetics Analysis (MEGA) for macOS. Mol Biol Evol 37: 1237–1239.

Stoecker DK, Li A, Coats W, Gustafson DE, Nannen MK (1997) Mixotrophy in the dinoflagellate *Prorocentrum minimum*. Mar Ecol Prog Ser 152: 1–12.

Su-Myat, Koike K (2013) A red tide off the Myanmar coast: Morphological and genetic identification of the dinoflagellate composition. Harmful Algae 27: 149–158.

Tamura K, Stecher G, Kumar S (2021) MEGA 11: Molecular Evolutionary Genetics Analysis Version 11. Mol Biol Evol 38: 3022–3027.

Taylor FJR, Waters RE (1982) Spring phytoplankton in the Subarctic North Pacific Ocean. Mar Biol 67: 323–335.

Telesh IV, Schubert H, Skarlato SO (2016) Ecological niche partitioning of the invasive dinoflagellate *Prorocentrum minimum* and its native congeners in the Baltic Sea. Harmful Algae 59: 100–111.

Tenorio C, Álvarez G, Perez-Alania M, Blanco JL, Paulino C, Blanco J, Uribe E (2022) Bloom of *Prorocentrum cordatum* in Paracas Bay, Peru. Diversity 14: 844.

Tillmann U, Gottschling M, Wietkamp S, Hoppenrath M (2023a) Morphological and phylogenetic characterisation of *Prorocentrum spinulentum*, sp. nov. (Prorocentrales, Dinophyceae), a small spiny species from the North Atlantic. Microorganisms 11: 271.

Tillmann U, Mitra A, Flynn KJ, Larsson ME (2023b) Mucus-trap-assisted feeding is a common strategy of the small mixoplanktonic *Prorocentrum pervagatum* and *P. cordatum* (Prorocentrales, Dinophyceae). Microorganisms 11: 1730.

Tillmann U, Wietkamp S, Gottschling M, Hoppenrath M (2023c) *Prorocentrum pervagatum* sp. nov. (Prorocentrales, Dinophyceae): A new, small, planktonic species with a global distribution. Phycol Res 71: 56–71.

Trick CG, Andersen RJ, Harrison PJ (1984) Environmental factors influencing the production of an antibacterial metabolite from a marine dinoflagellate, *Prorocentrum minimum*. Can J Fish Aquat Sci 41: 423–432.

Uchida T (1981) The relationships between *Prorocentrum micans*–growth and its ecological environment. Scientific Papers of the Institute of Algological Research, Faculty of Science, Hokkaido University 7: 17–76.

Uye S (1996) Induction of reproductive failure in the planktonic copepod *Calanus pacificus* by diatoms. Mar Ecol Prog Ser 133: 89–97.

Vershinin A, Moruchkov A, Morton SL, Leighfield TA, Quilliam MA, Ramsdell JS (2006) Phytoplankton composition of the Kandalaksha Gulf, Russian White Sea: *Dinophysis* and lipophilic toxins in the blue mussel (*Mytilus edulis*). Harmful Algae 5: 558–564.

Vrquez R, Hargraves PE (1995) Annual cycle of potentially harmful dinoflagellate in the Golfo de Nicoya, Costa Rica. Bull Mar Sci 57: 467–475.

Ward BA, Follows MJ (2016) Marine mixotrophy increases trophic transfer efficiency, mean organism size, and vertical carbon flux. Proc Natl Acad Sci USA 113: 2958–2963.

Wasmund N, Göbel J, Bodungen BV (2008) 100-years-changes in the phytoplankton community of Kiel Bight (Baltic Sea). J Mar Syst 73: 300–322.

Widdicombe CE, Eloire D, Harbour D, Harris RP, Somerfield PJ (2010) Long-term phytoplankton community dynamics in the Western English Channel. J Plankton Res 32: 643–655.

Wikfors GH, Fernandez E (2013) Induced bacteriovory in a declining culture of the mixotrophic dinoflagellate *Prorocentrum minimum* (Pavillard) Schiller. Int J Ecol 2013: 234372.

Xu N, Duan S, Li A, Zhang C, Cai Z, Hu Z (2010) Effects of temperature, salinity and irradiance on the growth of the harmful dinoflagellate *Prorocentrum donghaiense* Lu. Harmful Algae 9: 13–17.

Yang H, Lohmann G, Krebs-Kanzow U, Ionita M, Shi X, Sidorenko D, Gong X, Chen X, Gowan EJ (2020) Poleward shift of the major ocean gyres detected in a warming climate. Geophysical Research Letters 47: e2019GL085868.

Yokoi N, Matsuno K, Ichinomiya M, Nagasoe A, Nishino S, Onodera J, Inoue J, Kikuchi T (2015) Short-term changes in a microplankton community in the Chukchi Sea during autumn: consequences of a strong wind event. Biogeosciences 13: 913–923.